Molecular Biology of the Cell
Vol. 17, 3806–3818, September 2006

The Nup107-160 Nucleoporin Complex Is Required for Correct Bipolar Spindle Assembly[D]

Arturo V. Orjalo,* Alexei Arnaoutov,† Zhouxin Shen,* Yekaterina Boyarchuk,† Samantha G. Zeitlin,‡ Beatriz Fontoura,§ Steven Briggs,* Mary Dasso,† and Douglass J. Forbes*

Sections of *Cell and Developmental Biology and ‡Molecular Biology, Division of Biological Sciences, University of California-San Diego Medical School, La Jolla, CA 92093-0347; †Laboratory of Gene Regulation and Development, National Institute of Child Health and Human Development, National Institutes of Health, Bethesda, MD 20892-5431; and §Department of Cell Biology, University of Texas Southwestern Medical Center, Dallas, TX 75390-9039

Submitted November 18, 2005; Revised June 9, 2006; Accepted June 19, 2006
Monitoring Editor: Karsten Weis

The Nup107-160 complex is a critical subunit of the nuclear pore. This complex localizes to kinetochores in mitotic mammalian cells, where its function is unknown. To examine Nup107-160 complex recruitment to kinetochores, we stained human cells with antisera to four complex components. Each antibody stained not only kinetochores but also prometaphase spindle poles and proximal spindle fibers, mirroring the dual prometaphase localization of the spindle checkpoint proteins Mad1, Mad2, Bub3, and Cdc20. Indeed, expanded crescents of the Nup107-160 complex encircled unattached kinetochores, similar to the hyperaccumulation observed of dynamic outer kinetochore checkpoint proteins and motors at unattached kinetochores. In mitotic *Xenopus* egg extracts, the Nup107-160 complex localized throughout reconstituted spindles. When the Nup107-160 complex was depleted from extracts, the spindle checkpoint remained intact, but spindle assembly was rendered strikingly defective. Microtubule nucleation around sperm centrosomes seemed normal, but the microtubules quickly disassembled, leaving largely unattached sperm chromatin. Notably, Ran-GTP caused normal assembly of microtubule asters in depleted extracts, indicating that this defect was upstream of Ran or independent of it. We conclude that the Nup107-160 complex is dynamic in mitosis and that it promotes spindle assembly in a manner that is distinct from its functions at interphase nuclear pores.

INTRODUCTION

Communication between the nucleus and cytoplasm occurs through the nuclear pore complex (NPC; reviewed in Vasu and Forbes, 2001; Suntharalingam and Wente, 2003; Hetzer *et al*., 2005). At mitosis the metazoan nuclear pore disassembles into approximately a dozen subunits. The major subunit, both in size and complexity, is the nine-protein vertebrate Nup107-160 complex, which includes Nup160, Nup133, Nup107, Nup96, Nup85, Nup43, Nup37, Sec13, and Seh1 (Belgareh *et al*., 2001; Vasu *et al*., 2001; Cronshaw *et al*., 2002; Harel *et al*., 2003b; Devos *et al*., 2004; Loiodice *et al*., 2004). In yeast, a nearly identical complex exists (Siniossoglou *et al*., 1996, 2000; Teixeira *et al*., 1997; Lutzmann *et al*., 2002), lacking only the vertebrate Nup43 and Nup37 subunits for which there are no yeast counterparts.

Nuclear reconstitution in interphase *Xenopus* egg extracts depleted of the Nup107-160 complex produced nuclear envelopes with enclosed membranes, but completely devoid of nuclear pores (Harel *et al*., 2003b; Walther *et al*., 2003a). These studies suggest that the Nup107-160 complex is a central and early determinant in NPC assembly. Genetic studies in yeast indicate the complex plays a critical role in mRNA export (Doye *et al*., 1994; Heath *et al*., 1995; Li *et al*., 1995; Pemberton *et al*., 1995; Goldstein *et al*., 1996; Siniossoglou *et al*., 1996). In human cells, RNA interference (RNAi) and transfection of dominant-negative fragments of individual complex members have revealed that vertebrate mRNA export is similarly dependent upon this complex (Vasu *et al*., 2001; Boehmer *et al*., 2003; Harel *et al*., 2003b; Walther *et al*., 2003a).

The Nup107-160 complex has been localized at kinetochores in mammalian cells during mitosis (Belgareh *et al*., 2001; Harel *et al*., 2003b; Loiodice *et al*., 2004), and one of its constituents, Nup96, has also been found at the spindles and spindle poles (Enninga *et al*., 2003). These studies used different antibodies and experimental conditions. However, the function of this complex in these sites was not established. Deletion mutants in either *Saccharomyces cerevisiae* or *Schizosaccharomyces pombe* lacking the homologues of vertebrate Nup160, show significant defects in mitotic spindles (Aitchison *et al*., 1995; Bai *et al*., 2004). The mechanism through which the Nup107-160 complex may contribute toward spindle assembly is currently unknown.

Notably, other nucleoporins and transport factors also play a role in spindle assembly. The mammalian nucleoporin Nup358 (also called RanBP2) is a component of the

This article was published online ahead of print in *MBC in Press* (http://www.molbiolcell.org/cgi/doi/10.1091/mbc.E05–11–1061) on June 28, 2006.

[D] The online version of this article contains supplemental material at *MBC Online* (http://www.molbiolcell.org).

Address correspondence to: Douglass Forbes (DForbes@UCSD.edu).

Abbreviation used: NPC, nuclear pore complex.

cytoplasmic filaments of the interphase NPC (Vasu and Forbes, 2001; Suntharalingam and Wente, 2003). It is targeted to mitotic kinetochores with its binding partner, RanGAP1 (Joseph *et al*., 2002, 2004; Salina *et al*., 2003). RNAi-mediated depletion of Nup358 induces mitotic arrest with defective spindles (Salina *et al*., 2003; Joseph *et al*., 2004). Moreover, disruption of its targeting to kinetochores causes defects in the microtubule fibers connecting kinetochores to spindle poles (Arnaoutov *et al*., 2005). Additionally, the mRNA transport factor Rae1 is associated with microtubules in interphase HeLa cells and neurons (Kraemer *et al*., 2001). During mitosis, Rae1 localizes to the mitotic spindle, with enrichment at the spindle poles (Blower *et al*., 2005). In *Xenopus* mitotic extracts, Rae1 binds to the spindle in an RNA-containing complex, whose depletion disrupts microtubule nucleation and aster formation, among the earliest steps in spindle assembly (Blower *et al*., 2005). Rae1 has also been implicated in both *S. pombe* and vertebrate cells as a regulator of mitotic cell cycle progression (Whalen *et al*., 1997; Jeganathan *et al*., 2005). The extent to which other NPC-associated proteins may be involved in spindle assembly and function is an important question for future investigation.

Interestingly, some kinetochore proteins show a reciprocal localization: the Mad1, Mad2, and Mps1 proteins act at kinetochores during mitosis, as part of the spindle checkpoint pathway that prevents premature anaphase onset until all chromosomes are attached to the spindle and aligned on the metaphase plate. During interphase, however, these proteins associate with yeast and vertebrate nuclear pores (Campbell *et al*., 2001; Iouk *et al*., 2002; Liu *et al*., 2003; Stukenberg and Macara, 2003). In budding yeast, there is evidence that nuclear pore association of Mad1 and Mad2 is linked to the spindle checkpoint (Iouk *et al*., 2002), but not essential for checkpoint activation (Kastenmayer *et al*., 2005). This association seems to be controlled by the small GTPase Ran in both yeast and vertebrate cells (Quimby *et al*., 2005).

Indeed, Ran may be a functional connector between many of these events. A chromatin-bound Ran-GEF (RCC1) produces Ran-GTP, which plays a critical role in directing spindle assembly around chromosomes during mitosis (Carazo-Salas *et al*., 1999; Kalab *et al*., 1999; Ohba *et al*., 1999; Wilde and Zheng, 1999; Zhang *et al*., 1999). Elevation of Ran-GTP levels in mitotic *Xenopus* egg extracts causes the assembly of microtubules in a chromosome-independent manner, which in turn become rearranged over time into structures resembling spindles. It is widely believed this effect results from the capacity of Ran-GTP to release inhibitory interactions between mitotic spindle assembly factors and transport receptors (Gruss *et al*., 2001; Nachury *et al*., 2001; Wiese *et al*., 2001; Trieselmann *et al*., 2003; Tsai *et al*., 2003; Ems-McClung *et al*., 2004). Under normal circumstances, this function might be limited to the immediate vicinity of chromosomes due to the restricted localization of RCC1 (Askjaer *et al*., 2002; Kalab *et al*., 2002; Trieselmann and Wilde, 2002; Li and Zheng, 2004; Caudron *et al*., 2005; reviewed in Harel and Forbes, 2004; Clarke, 2005). Ran-GTP also plays crucial roles in the spindle checkpoint (Arnaoutov and Dasso, 2003), centrosomal function (Di Fiore *et al*., 2003; Keryer *et al*., 2003; Di Fiore *et al*., 2004), postmitotic nuclear assembly (Zhang *et al*., 1999; Hetzer *et al*., 2000; Zhang and Clarke, 2000, 2001; Bamba *et al*., 2002; Hetzer *et al*., 2002; Harel *et al*., 2003a; Walther *et al*., 2003b), and interphase nuclear transport (Macara, 2001). It may well be that evolution has sought the most parsimonious option, using the dual localization of nucleoporins and spindle checkpoint proteins, which are found at pores and kinetochores, because both are subject to Ran control.

In the present study, we have investigated the mitotic role of the Nup107-160 nucleoporin complex. Immunofluorescence in mammalian cells and *Xenopus* egg mitotic extracts revealed that the Nup107-160 complex, in addition to localizing to kinetochores, localizes to the spindle poles and within the spindle. Nup107-160 complex behavior in mammalian cells strikingly resembled the behavior of a subset of spindle checkpoint proteins, as did the accumulation of the Nup107-160 complex at unattached kinetochores. Although the complex did not seem to be essential for spindle checkpoint signaling, the Nup107-160 complex was essential for mitotic spindle assembly in vitro. These findings clearly indicate that the Nup107-160 complex is highly dynamic during mitosis and that it has mitotic functions that are distinct from its interphase roles in NPC structure and nucleocytoplasmic trafficking.

MATERIALS AND METHODS

Constructs, Immunoprecipitation, and Antibodies

A full-length cDNA encoding 375 aa of *Xenopus* Nup43 was prepared using reverse transcription of XL177 total RNA. The oligonucleotides used in the PCR amplification were derived using the extreme 5′ and 3′ aa sequences of the GenBank *Xenopus* clones (GenBank/EMBL/DDBJ accession nos. BX843375 and BG016768). After the cDNA was cloned into pET-28a, the recombinant protein was expressed in *Escherichia coli* Rosetta (DE3), purified on Ni-NTA agarose (QIAGEN, Valencia, CA), and used to immunize a rabbit. Antibodies were affinity purified against the same xNup43 protein coupled to CNBr-activated Sepharose (GE Healthcare, Little Chalfont, Buckinghamshire, United Kingdom).

A cDNA encoding of *Xenopus* Nup37 (aa 1–267) was reverse transcription-PCR cloned using 5′ and 3′ oligonucleotides derived from GenBank/EMBL/DDBJ accession no. CA788183 and total XL177 RNA. The cDNA was amplified by PCR, cloned into pET-28a, and expressed. Antibodies were raised and affinity purified against the same *Xenopus* protein.

Expression of RanQ69L from pET-28a in *E. coli* Rosetta (DE3) was induced by the addition of 1 mM isopropyl-β-D-thiogalactopyranoside for 5 h at 37°C. The cells were lysed by sonication, and the protein was purified on Ni-NTA agarose. The eluted fractions containing RanQ69L were then dialyzed into phosphate-buffered saline (PBS) overnight at 4°C, concentrated using an Amicon Ultra-4 centrifugal filter device (Millipore, Billerica, MA), and loaded with GTP as described previously (Kutay *et al*., 1997). RanQ69L loaded with GTP was finally dialyzed into PBS/5% glycerol for 4 h and concentrated further using an Ultrafree-0.5 centrifugal filter device (Millipore).

Immunoprecipitation was done using *Xenopus* egg cytosol prepared as described previously (Shah *et al*., 1998). Affinity-purified IgG against hNup133 and xNup43 or nonimmune rabbit IgG (5 μg; Calbiochem/EMD Biosciences, San Diego, CA) were coupled to 20 μl of nProtein A-Sepharose (GE Healthcare). The beads were incubated in egg extract (20 μl) added to 500 μl of PBS (2 h; 4°C), washed three times in PBS, eluted with 0.1 M glycine, pH 2.5 (20 μl), and neutralized with 0.1 volume of 1.0 M Tris, pH 8.0. Samples (5 μl) were loaded, resolved by SDS-PAGE, and immunoblotted.

Antibodies against the following proteins were used: rabbit polyclonal antibodies against Bub1, BubR1, and Mad2 (kindly provided by R. H. Chen, Institute of Molecular Biology, Academia Sinica, Taipei, Taiwan), monoclonal antibodies against human CENP-B (kindly provided by D. Cleveland, Ludwig Institute for Cancer Research, University of California-San Diego) and human Nup62 (BD Transduction Laboratories, Lexington, KY), and rabbit polyclonal antibodies against *Xenopus* NuMA (kindly provided by D. Cleveland), hNup160, mNup85, hNup133 (Harel *et al*., 2003a), and human Nup96 (Fontoura *et al*., 1999).

Preparation of Mitotic Extracts for Spindle Assembly, Immunodepletion, and Antibody Addition

Frogs for mitotic (i.e., cytostatic factor [CSF] arrested) extract preparation were primed with 100 U of pregnant mare serum gonadotropin (Calbiochem) and placed in water containing 2 g/l NaCl for at least 48 h. Sixteen to 18 h before extract preparation, the primed frogs were induced to ovulate with 500 U of human chorionic gonadotropin (Sigma-Aldrich, St. Louis, MO) and put into individual buckets containing modified Ringer's solution (MMR). They laid their eggs overnight at 16°C, which were then collected in 250-ml beakers the next morning. After removing most of the MMR from the good batches of eggs, a 2% cysteine solution was added for dejellying. Eggs that seemed activated were constantly removed by a transfer pipette (Fisher Scientific, Pittsburgh, PA). The dejellied eggs were then washed three or four times with CSF-XB (Desai *et al*., 1999). Using a cut-tip transfer pipette, the eggs were

drawn up and slowly dropped into a 14-ml polypropylene round-bottomed tube (BD Biosciences Discovery Labware, Bedford, MA) containing 1 ml CSF-XB + aprotinin/leupeptin and cytochalasin B. After the excess buffer was removed from the top of the eggs, the tubes were spun for 20 s at setting 4 in a clinical centrifuge and then 15 s at setting 6. Buffer from the top of the eggs was gently removed, and the tubes were spun in the HB-6 rotor in the ultracentrifuge at 10,000 rpm for 15 min at 16°C. The cytoplasmic layer was removed with an 18-guage needle on a 3-ml syringe and gently drawn out. The needle was then removed and the extract transferred to a 14-ml polypropylene round-bottomed tube on ice. Finally, additional aprotinin/leupeptin and cytochalasin B was added as well an ATP energy mix.

Where indicated, rhodamine-labeled tubulin was added at a final concentration of 25 μg/ml. Checkpoint extracts were prepared by incubation with 20 μg/ml nocodazole for 40 min. Ran asters were generated by the addition of RanQ69L to extracts at a concentration of 25 μM. When used, sperm nuclei were added at a final concentration of 500 nuclei/μl.

For immunodepletion, a combined 400 μg of affinity-purified antibodies against hNup133 and xNup43 or an equal amount of nonimmune rabbit IgG were bound to 60 μl of nProtein A-Sepharose overnight. The bound antibody beads were blocked with 20 mg/ml bovine serum albumin in PBS buffer and washed twice with PBS and three times with CSF-XB. CSF-arrested extract (100 μl) was added to 30 μl of antibody or rabbit IgG beads and tumbled for 30 min (23°C) for two consecutive depletions. For the analysis of Ran asters and spindles in mock and depleted extracts, 20-μl reactions were fixed and spun onto coverslips as described previously (Desai *et al*., 1999).

A different protocol was used to analyze mitotic chromatin without preserving the spindles. Twenty microliters of each reaction was first diluted fivefold with 0.8× CSF-XB containing 250 mM sucrose and then mixed with 1 ml of fixation buffer (0.8× CSF-XB, 250 mM sucrose, 4% paraformaldehyde) for 30 min at room temperature. The reactions were then layered onto a 40% glycerol cushion in 0.8× CSF-XB + 0.1% Triton X-100 and pelleted onto coverslips for 10 min at 18°C at 6000 × *g*. They were then processed for immunofluorescence as described previously (Harel *et al*., 2003a). Cycling extracts were prepared as described previously (Desai *et al*., 1999).

For antibody addition experiments, sperm chromatin was first added to CSF extracts, which had been induced to enter interphase by the addition calcium chloride (0.4 mM final). The chromatin packages then formed nuclear structures. These extracts containing nuclei were then reconverted to mitosis by the addition of an equal volume of fresh CSF mitotic extract. This extract contained either affinity-purified anti-Nup133 or -Nup43 antibodies or nonimmune rabbit IgG. The antibody concentration in the final reactions was 1 mg/ml. To quantitate the relative density of microtubules in the resultant spindles, images were acquired using a 63× objective and analyzed using Imaris imaging software (Bitplane, St. Paul, MN). The *z*-axis stacks of fluorescent images, corresponding to slices along the long axis of the spindle, were examined visually to determine the medial plane of the spindle, where microtubule density would be greatest. Within the appropriate stack, a 100 × 100 pixel region was chosen roughly halfway between the chromosomes and spindle poles. The fluorescence within this region was integrated. Background was determined by measuring a corresponding 100 × 100 pixel region in an adjoining area of the same field lacking microtubules or chromatin. The background was subtracted to provide the final measurement of fluorescence intensity provided in Supplemental Table 3.

For assessing the chromatin recruitment of checkpoint proteins under spindle checkpoint conditions and the sensitivity of this to RCC1/RanGEF, experiments were performed as described previously (Arnaoutov and Dasso, 2003).

Cell Culture and Immunofluorescence

HeLa cells were grown in DMEM supplemented with 10% fetal calf serum. In Figure 2, HeLa cells were first permeabilized for immunofluorescence with PHEM buffer (60 mM PIPES, 20 mM HEPES, pH 6.9, 10 mM EGTA, 4 mM $MgSO_4$, 0.1% Triton X-100) for 5 min and then fixed with −20°C methanol for 10 min. The cells were then processed for immunofluorescence as described previously (Harel *et al*., 2003a) with the appropriate primary and secondary antibodies. Coverslips were mounted with VECTASHIELD (Vector Laboratories, Burlingame, CA), and visualized with a Zeiss Axioskop fluorescence microscope (Carl Zeiss, Thornwood, NY).

Images collection for Figure 4 was performed at the University of California-San Diego Cancer Facility in the laboratory of Dr. James Feramisco on a Deltavision deconvolution microscope (Applied Precision, Issaquah, WA).

Mass Spectroscopy Analysis of Mitotic and Interphase Nup107-160 Complex

To study the composition of the Nup107-160 complex in interphase and mitotic *Xenopus* extract, the complex was immunoprecipitated with anti-hNup133 or anti-xNup43 antibodies as follows: affinity-purified antibodies (5 μg) or nonimmune rabbit IgG (5 μg; Calbiochem/EMD Biosciences) were covalently coupled to 20 μl of nProtein A-Sepharose (GE Healthcare) with dimethyl pimelimidate. Each set of antibody beads was incubated with mitotic CSF egg extract (20 μl in 500 μl of CSF-XB buffer) or the identical extract converted to interphase by addition of calcium chloride and incubation for 1 h at room temperature (20 μl in 500 μl of CSF-XB buffer). The six immunoprecipitation reactions were incubated for 1 h at 23°C, washed three times in CSF-XB buffer, and bound proteins eluted with 0.1 M glycine, pH 2.5 (20 μl). The mixtures were neutralized with 0.1 volumes of 1.0 M Tris, pH 8.0. The immunoprecipitated proteins were reduced and alkylated using 2 mM tris(2-carboxyethyl)phosphine (AC36383; Fisher Scientific) at 37°C for 30 min and 5 mM iodoacetamide (AC12227; Fisher Scientific) at 37°C in dark for 30 min, respectively. The proteins were digested with 0.5 mg of trypsin (03 708 969 001; Roche Diagnostics, Indianapolis, IN) overnight.

A reverse phase gradient from 0 to 80% acetonitrile at 300 nl/min flow rate was used to elute the peptides from a self-packed C18 capillary column (20 cm long × 100 mM i.d.) by using an Agilent 1100 quaternary high-performance liquid chromatography pump (Agilent Technologies, Palo Alto, CA). Eluted peptides were directly analyzed by a Thermo Electron (Waltham, MA) LTQ ion trap mass spectrometer. About 20,000 tandem mass spectrometry (MS/MS) spectra were collected for each sample.

The raw data were extracted and searched using Spectrum Mill (version A.03.01.037a SR1; Agilent Technologies). MS/MS spectra with a sequence tag length of 1 or more were searched against the National Center for Biotechnology Information (NCBI, Bethesda, MD) dbEST database (version 7/12/2005) limited to *Xenopus* taxonomy (1,344,320 expressed sequence tag [EST] sequences). The enzyme parameter was limited to full tryptic peptides with a maximum miscleavage of 2. All other search parameters were set to SpectrumMill's default settings. Search results for individual spectra were automatically validated using the following filtering criteria: 1) protein details mode: score >9 for 1+ and 2+ peptides and score >11 for 3+ peptides; and 2) peptide mode: score >11 for 1+, >12 for 2+ and score >13 for 3+ peptides. The false-positive rate for such criteria was estimated by searching the same data set against a combined forward-reverse database of NCBI nonredundant protein database limited to human, fish, and reptile taxonomies. Among the autovalidated 97 proteins and 314 peptides, two proteins were from the reverse sequence database. And both of them are single-peptide hits. Thus, the false-positive rate of our filtering criteria is 1% spectra and 4% protein. Only proteins with at least two unique peptides were selected for comparative analysis between different samples.

Quantitation of Kinetochore Staining with Anti-Nup133 Antibodies

Measurements of kinetochore fluorescence in Supplemental Table 2 were obtained as described previously (Hoffman *et al*., 2001), by using Imaris imaging software. Images were acquired using a 63× objective and analyzed without deconvolution. The best in-focus images of individual kinetochore were determined by stepping through the *z*-axis stacks of corresponding fluorescence images visually. Computer-generated 9 × 9 and 13 × 13 pixel regions were centered over each kinetochore. The former region corresponded was typically large enough to contain essentially all kinetochore fluorescence. The outer region was chosen to be more than double the area of the inner region but to exclude significant fluorescence from adjacent kinetochores. The background component of the 9 × 9 pixel region was determined by subtracting the integrated value of that region from the larger 13 × 13 pixel region. The resulting measurement was scaled in proportion to the area of the 9 × 9 pixel region. The scaled measurement was subtracted from the integrated value of the 9 × 9 pixel region, to yield the final value for kinetochore fluorescence. Average values of kinetochore fluorescence were calculated from 20 kinetochores for each experimental condition.

RESULTS

The Xenopus Nup107-160 Complex Contains New Members Nup43 and Nup37

The human Nup107-160 complex contains nine members, including two recently identified members that have not been described previously in *Xenopus*, Nup43 and Nup37 (Belgareh *et al*., 1998; Vasu *et al*., 2001; Cronshaw *et al*., 2002; Harel *et al*., 2003b; Loiodice *et al*., 2004). To better use the powerful biochemistry of the *Xenopus* egg extract system for investigation of Nup107-160 complex function, we cloned and raised antibodies to *Xenopus* and human Nup43 and Nup37 (Figure 1, A–C; see *Materials and Methods*). We found that the *Xenopus* Nup107-160 complex in eggs contains these proteins. Anti-xNup43 and anti-hNup133 antisera each coimmunoprecipitate Nup160, Nup133, Nup85, Sec13, Nup43, and Nup37 (Figure 1, E and F). Furthermore, mass spectroscopy analysis of Nup43 and Nup133 immunoprecipitates indicate that all nine Nup107-160 complex members are present (Supplemental Table 1).

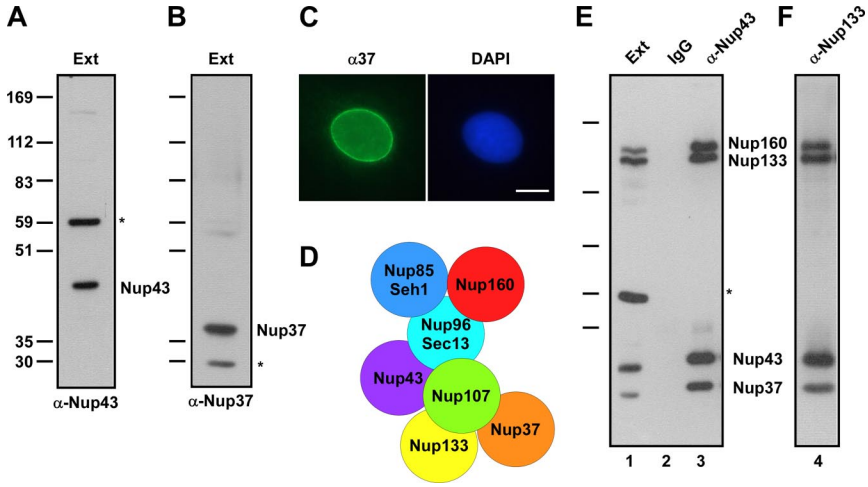

Figure 1. xNup43 and xNup37 are components of the *Xenopus* Nup107-160 complex. (A) An antibody raised to amino acids 1–375 of *Xenopus* Nup43 recognizes two bands in *Xenopus* interphase extract. The lower band is Nup43, and the higher band labeled with the asterisk is a cross-reacting protein. (B) An antibody raised to amino acids 1–267 of *Xenopus* Nup37 recognizes two bands in *Xenopus* interphase extract. The higher band is Nup37, and the lower band labeled with the asterisk is a cross-reacting protein. (C) Immunofluorescence on interphase XL177 *Xenopus* cells was performed with anti-xNup37 antibody (left), which localizes in a punctate pattern on the nuclear rim, characteristic of a nuclear pore stain. Right, DNA stained with 4,6-diamidino-2-phenylindole (DAPI). Bar, 10 μm. (D) Schematic of the nine-member *Xenopus* Nup107-160 complex is shown. Because the nearest neighbors of Nup43 and Nup37 are unknown, they are placed arbitrarily in the subcomplex. (E) Nup37 and Nup43 are members of the *Xenopus* Nup107-160 nuclear pore subcomplex. Anti-Nup43 antibody immunoprecipitates Nup43 as well as the other members of the Nup107-160 complex, including Nup160, Nup133, and Nup37, from interphase extract (lane 3). Note that the cross-reacting band indicated by the asterisk does not coimmunoprecipitate with the Nup107-160 complex. (F) Anti-Nup133 antibody reciprocally immunoprecipitates Nup43 as well as other complex members, such as Nup160 and Nup37.

We conclude that, as in mammals, the *Xenopus* Nup107-160 complex, shown in Figure 1D, contains nine proteins: Nup160, Nup133, Nup107, Nup96, Nup85, Sec13, Seh1, Nup43, and Nup37. Interestingly, we see no major differences in the subunits immunoprecipitated from interphase or mitotic *Xenopus* extracts (Supplemental Table 1), suggesting that this represents a constitutive pore subcomplex that is present throughout the cell cycle.

The mammalian Nup107-160 Complex Localizes to Prometaphase Spindles and Spindle Poles

Previous analysis observed that a small fraction of the Nup107-160 complex (~5%) localizes to kinetochores during mitosis (Belgareh *et al*., 2001; Harel *et al*., 2003b; Loiodice *et al*., 2004). In these studies, however, distribution of the remaining Nup107-160 complex throughout the mitotic cell effectively obscured other potential sites of localization. To reveal additional sites of localization, we performed immunofluorescence on mitotic HeLa cells, using a protocol designed to release soluble Nup107-160 complexes. As expected, the Nup107-160 complex was present on kinetochores at all stages of mitosis (Figure 2A, left). However, immunofluorescence in the absence of soluble cytoplasmic proteins also showed clear localization of Nup133 to the spindle poles and proximal spindle microtubules (Figure 2A). Polar localization was similarly observed using antibodies against other Nup107-160 complex members, including Nup85 (Figure 2B), Nup96 (Figure 2C), and Nup160 (Figure 2C). Antisera directed against nucleoporins that are not members of the Nup107-160 complex, i.e., Nup93 and Nup62, did not stain kinetochores or spindles at any stage of mitosis (Figure 2C).

Spindle pole staining could be seen specifically in prometaphase, as judged from the incomplete alignment of the chromosomes onto the metaphase plate. This polar localization of the Nup107-160 complex was not observed in metaphase or anaphase cells (Figure 2A). The narrow time window of Nup107-160 complex localization on spindles in mammalian cells suggested an explanation for why the majority of these nucleoporins (Nup133, Nup85, and Nup160) had not been previously observed at the spindle poles by immunofluorescence (Belgareh *et al*., 2001; Loiodice *et al*., 2004) as well as an explanation for why the spindle localization of Nup96 has been controversial (Enninga *et al*., 2003; Loiodice *et al*., 2004). The bulk of those studies concentrated on metaphase and anaphase cells, beyond the interval at which the complex is concentrated on spindles and poles; they would thus have found only negligible localization of this complex on those structures.

To confirm definitively the localization of the Nup107-160 complex at spindle poles, we performed simultaneous immunofluorescence with antisera to Nup133 and NuMA, a nuclear protein that is an established component of mitotic spindle poles (Merdes *et al*., 1996, and references therein). We found nearly identical localization of NuMA and Nup133 in prometaphase cells in the region of the spindle poles (Figure 2D). Interestingly, the distribution of the Nup107-160 complex is highly reminiscent of the behavior of a subset of the spindle checkpoint proteins during early mitosis. Specifically, Mad1, Mad2, Bub3, and Cdc20 move along microtubules from the kinetochores, accumulating on spindle poles at prometaphase (Howell *et al*., 2004). They are subsequently lost from kinetochores, spindles, and poles in metaphase. When we used anti-Mad2 antisera to stain HeLa cells, we observed a prometaphase spindle pole stain (Figure 2C, right), identical to that seen with our anti-Nup107-160 complex antisera. We conclude that the Nup107-160 complex is much more dynamic in mitosis than had been thought and that it is found at multiple locations within the mitotic spindle, correlated with the extent of spindle formation.

The Nup107-160 Complex Localizes to Spindles and Ran Asters in Mitotic Xenopus Extracts

To address Nup107-160 complex mitotic function in a system more amenable to manipulation, we next used *Xenopus* mitotic extracts. *Xenopus* eggs are naturally arrested in meiotic metaphase. When lysed in the presence of the calcium chelator EGTA, the resulting low Ca^{2+} concentration maintains the extract, termed a CSF-arrested extract, within metaphase (Murray, 1991; Heald *et al*., 1996; Desai *et al*., 1999). When sperm chromatin is added to a CSF extract, microtu-

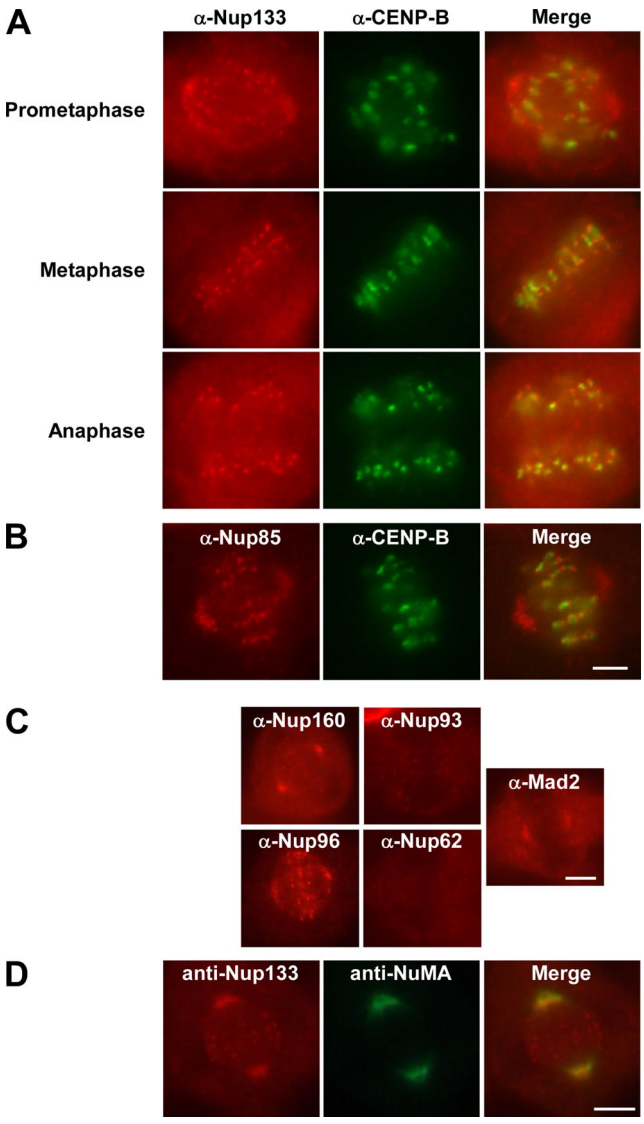

Figure 2. The Nup107-160 complex localizes to kinetochores, spindle poles, and microtubules during prometaphase. (A and B) HeLa cells were prepared for immunofluorescence as described in *Materials and Methods* and stained with affinity-purified anti-hNup133 (red, A), affinity-purified anti-mNup85 (red, B), or an anti-hCENP-B monoclonal antibody (mAb) (green, A and B). A merge is shown in the right panels (A and B). Whereas CENP-B and the Nup107-160 complex were present throughout mitosis on centromeres and kinetochores, respectively, only the Nup107-160 complex was found at the spindle poles and proximal microtubules during prometaphase (A, prometaphase). Nup107-160 complex spindle pole localization was greatly diminished or absent after cells entered metaphase (A, metaphase and anaphase). Bar, 4 μm. (C) Immunofluorescence with anti-hNup160 and anti-hNup96 antibodies on HeLa cells stained the spindle poles during prometaphase (red, far left), identical to the localization seen for Nup133 and Nup85 in A and B. Immunofluorescence with affinity-purified anti-hNup93 polyclonal antibody or an anti-hNup62 mAb does not give a spindle stain. Affinity-purified antisera to Mad2, an outer kinetochore checkpoint protein found at the spindle poles and proximal microtubules during prometaphase (Howell *et al.*, 2004), shows localization identical to that of the Nup107-160 complex at that stage of the cell cycle (far right). Bar, 5 μm. (D) Nup133 colocalizes with NuMA in prometaphase HeLa cells. In cells prepared for immunofluorescence with affinity-purified anti-hNup133 and affinity-purified anti-xNuMA antisera, the localization of Nup133 and NuMA overlap in the spindle pole area in prometaphase cells. Nup133 is also found at the kinetochores and free in the cytoplasm. Bar, 5 μm.

bules assemble around each set of sperm chromosomes to form bipolar spindles within ~60 min. If rhodamine-labeled tubulin is present during the reaction, microtubules can be easily observed organized into bipolar spindles. Alternatively, spindles can be formed around fully replicated chromosomes with duplicated centrosome pairs in "cycled" extracts. In this case, CSF extracts are converted to interphase through the addition of calcium, and added sperm chromatin is allowed to form nuclei and undergo DNA replication for 60 min. When replication is complete, the extracts are induced to reenter mitosis through the addition of an equal volume of fresh CSF extract. The addition of CSF extract under these conditions normally promotes nuclear envelope breakdown, chromatin condensation, and spindle formation.

We first determined whether the Nup107-160 complex associated with in vitro assembled *Xenopus* spindles in cycled egg extracts containing added sperm chromatin and rhodamine-labeled tubulin. After fixation, the spindles were centrifuged onto coverslips. Immunofluorescence was performed with affinity-purified antibodies to hNup133, xNup43, hNup62 (a noncomplex nucleoporin) as well as control rabbit IgG antibodies. Both Nup133 and Nup43 were clearly detected throughout the assembled spindles (Figure 3A). Neither anti-Nup62 nor control rabbit IgG antibodies, however, stained *Xenopus* spindles (Figure 3A). Similar to these spindle localization results, the Nup107-160 complex localized at foci of RanGTP-induced microtubule asters formed directly in CSF extracts (Supplemental Figure 1). Together, our results suggest that the Nup107-160 complex is localized to mitotic spindles in both human somatic cells and *Xenopus* egg extracts. Moreover, these findings show that Nup107-160 recruitment to asters is not dependent upon their association with chromosomes.

Because of the high concentration of Nup107-160 complex proteins on spindles (Figure 3A), it was difficult to observe kinetochore staining above the bright spindle stain. However, in the occasional spindle with fainter anti-Nup133 stain, we clearly observed bright foci at the midplane of the spindle (Figure 3B). For purely technical reasons, it was not possible to confirm the identity of these foci as kinetochores by immunostaining. However, given their localization, paired appearance, and the high degree of conservation between the *Xenopus* and human Nup107-160 complexes, these sites are likely to be *Xenopus* kinetochores (also see Figure 4A) Together, the data indicate that the Nup107-160 complex is present throughout in vitro reconstituted spindles, in a manner that may be analogous to its localization on mammalian prometaphase spindles.

Recruitment of the Nup107-160 Complex to Unattached Kinetochores

Given the dynamic nature of Nup107-160 complex localization through mitosis, we wished to determine whether the amount of Nup107-160 complex on kinetochores is dependent upon microtubule attachment. We addressed this question by assembling kinetochores in vitro using sperm chromatin in *Xenopus* CSF extract plus or minus the microtubule depolymerizing agent, nocodazole (see Hoffman *et al.*, 2001), and references therein). After 40 min, the chromatin was centrifuged onto coverslips and immunofluorescence was performed with antisera directed against Nup37 and against checkpoint protein Bub1. As expected, significantly more Bub1 was recruited to kinetochores in the presence of nocodazole than in untreated extracts (Figure 4A, top and bottom center panels). Nup37 also showed an increase in intensity at kinetochores in nocodazole-treated extracts (Fig-

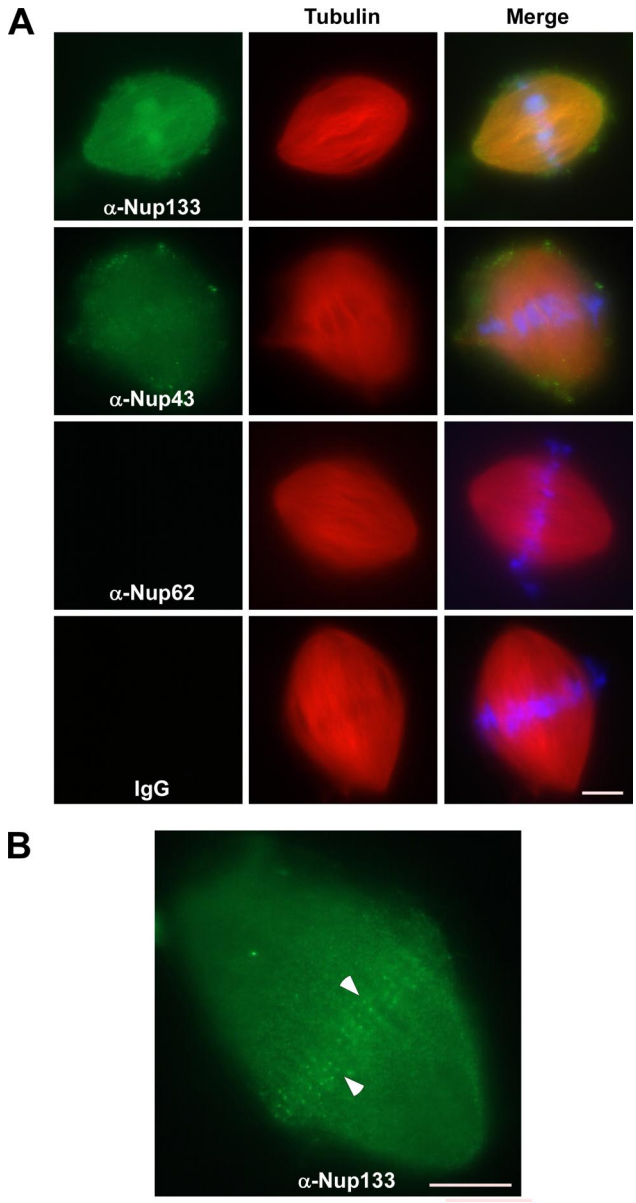

Figure 3. The Nup107-160 complex localizes to in vitro-assembled mitotic spindles. (A) Demembranated sperm chromatin and rhodamine-labeled tubulin were added to *Xenopus* CSF extracts. The reactions were induced to enter interphase through addition of 0.4 mM calcium chloride. After 1 h, the reactions were returned to mitosis by the addition of an equal volume of fresh CSF extract, and allowed to form spindles for 60 min. Reactions were fixed with formaldehyde, then the spindles were centrifuged onto coverslips, postfixed in methanol, and processed for immunofluorescence. The presence or absence of Nup133 (green, first row), Nup43 (green, second row), Nup62 (green, third row), or IgG (green, bottom row) on spindles was detected with the same affinity-purified antisera used in Figure 1. Presence of rhodamine-labeled tubulin (red, all rows), and DAPI-stained chromosomes (blue, all rows) is also shown. The right-most panels contain the merged images. Bar, 10 μm. (B) The staining of the in vitro assembled spindles by anti-Nup133 and Nup43 shown in A most often obscures concurrent kinetochore staining. However, occasional views reveal bright foci of kinetochore staining (indicated by arrowheads). An anti-Nup133 stain is shown. Bar, 10 μm.

ure 4A, top and bottom left). Although it is formally possible that this increased staining intensity may result from conformational changes within the complex that allow better antibody recognition, we do not believe that this is the case; very similar increases in staining intensity were consistently observed using multiple independent antisera directed against different complex members. Rather, we believe that the increased staining in nocodazole-treated extracts suggests increased Nup107-160 complex recruitment to unattached kinetochores in vitro.

To examine Nup107-160 complex recruitment onto unattached kinetochores in somatic cells, we treated HeLa cells for 2 h with nocodazole and stained with antibodies directed against Nup133. We found that more Nup133 was recruited to kinetochores in nocodazole-treated cells (Figure 4B, right) than in untreated cells (Figure 4B, left). Analysis of untreated and nocodazole-treated mitotic cells by using methods described by Hoffman *et al*. (2001) indicated a measurable (1.8-fold) increase in kinetochore staining intensity with nocodazole (Supplemental Table 2). Similar to the in vitro observations, this finding indicates that the Nup107-160 complex association to kinetochores is sensitive to microtubule attachment. Notably, nocodazole also caused Nup133, and presumably the entire Nup107-160 complex, to assemble as expanded crescents and rings were observed around kinetochores (Figure 4B, right, also see inset). A similar morphological change at unattached kinetochores of nocodazole-treated cells is characteristic of a subset of dynamic outer kinetochore proteins, including BubR1, Mad2, dynein, and CENP-E (Hoffman *et al*., 2001; Maiato *et al*., 2004).

The Xenopus Nup107-160 Complex Is Not Required for Spindle Checkpoint Activation

Given the similarities between Nup107-160 complex and spindle checkpoint proteins in their recruitment to unattached kinetochores, we wished to determine whether this complex plays a role in the checkpoint. To address this question, sperm chromatin and nocodazole were added to mock-depleted or Nup107-160 complex-depleted CSF extracts (Figure 5). After 40 min, the mitotic chromosomes and associated structures were centrifuged onto coverslips by using conditions that spread the DNA for better kinetochore analysis (Arnaoutov and Dasso, 2003). It should be noted that under these conditions, mitotic spindles and related microtubule structures are not well maintained.

Immunofluorescence on chromatin showed that the Bub1, BubR1, and Mad2 spindle checkpoint proteins were present on kinetochores in mock-depleted, nocodazole-treated egg extracts (Figure 5A, Noc/Mock). Strikingly, an identical pattern of checkpoint protein loading onto kinetochores was seen in Nup107-160 complex-depleted mitotic extracts (Figure 5A, Noc/D107-160). This loading could also be observed by biochemically analyzing centrifuged chromatin derived from mitotic reactions performed under the same experimental conditions. Immunoblotting of such chromatin with anti-Bub1 and anti-Mad2 antisera revealed that both mock- and Nup107-160-depleted extracts loaded spindle checkpoints onto chromatin/kinetochores in identical amounts (Figure 5B, lanes 1 and 3).

The addition of nocodazole to CSF extracts containing high concentrations of sperm chromatin results in the presence of unattached kinetochores, which are detected by the spindle checkpoint pathway and induce mitotic arrest (Minshull *et al*., 1994). As a result, such checkpoint arrested extracts do not exit from mitosis when CSF arrest is released with Ca^{2+}. The maintenance of this arrest can be monitored both through chromosome morphology and through the degradation of key mitotic regulators, such a cyclin B. We examined whether checkpoint arrest was induced normally in the

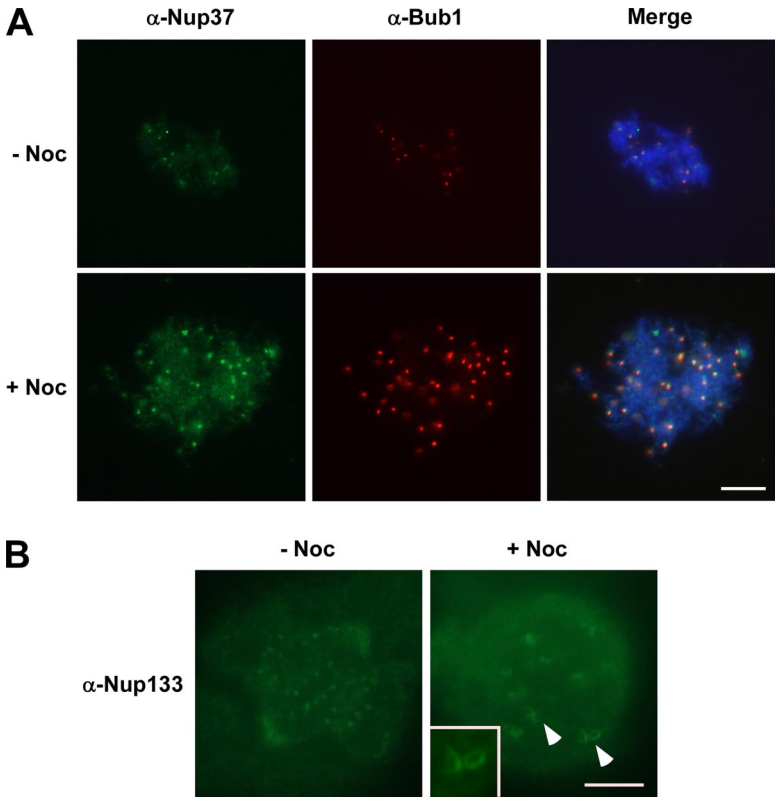

Figure 4. The Nup107-160 complex shows increased accumulation on unattached kinetochores. (A) Mitotic (CSF) extract was incubated with demembranated sperm chromatin for 40 min at 23°C with (bottom) or without (top) nocodazole. Mitotic chromosomes were collected and spread by centrifugation onto coverslips and then analyzed by indirect immunofluorescence with antibodies to *Xenopus* Nup37 (green) and Bub1 (red). The chromosomal DNA was stained with DAPI. Note that these conditions do not maintain spindle structure. Both Nup37 and BubR1 staining of kinetochores increases greatly. Bar, 10 μm. (B) HeLa cells were treated with nocodazole for 2 h before performing immunofluorescence by using affinity-purified anti-hNup133 antisera. The amount of the Nup107-160 complex, visualized with affinity-purified anti-hNup133 antisera, increased greatly giving large crescents, and ring structures typical of those outer kinetochore proteins that are affected by microtubule disassembly. Bar, 5 μm.

absence of the Nup107-160 complex (Figure 5, C and D). Both control and Nup107-160 complex-depleted extracts treated with dimethyl sulfoxide (DMSO) exited mitosis normally, as demonstrated by the degradation of cyclin B protein. Control extracts formed nuclei in the subsequent interphase, whereas the depleted extracts showed defects in nuclear assembly similar to those demonstrated previously (Harel *et al.*, 2003b; Walther *et al.*, 2003a). Notably, both control and Nup107-160 complex-depleted extracts showed mitotic arrest in response to the addition of nocodazole, with no evident change in condensed chromatin morphology or degradation of cyclin B. These results clearly indicate that the spindle assembly checkpoint does not absolutely require the Nup107-160 complex for its activation.

Finally, elevated levels of Ran-GTP can inactivate the spindle checkpoint in nocodazole treated extracts and release Mad2 and Bub1 from kinetochores (Arnaoutov and Dasso, 2003). This effect can be observed through the addition of exogenous RCC1, which promotes increased nucleotide exchange on Ran. Given the relationship between Ran and the NPC during interphase, we wondered whether this mechanism was still functional in the absence of the Nup107-160 complex. To address this question, we added RCC1 protein to nocodazole-treated mock- and Nup107-160 complex-depleted extracts and monitored release of the checkpoint proteins from the kinetochores. As shown in Figure 5B, release of Bub1 and Mad2 from chromatin was identical in the presence (lane 2) or absence (lane 4) of the Nup107-160 complex. Although we cannot rule out the possibility that the very small amount of Nup107-160 complex remaining in depleted extracts is sufficient for normal spindle checkpoint activity, our current observations indicate that Nup107-160 complex is not required in large amounts for recruitment of checkpoint proteins to unattached kinetochores, for the activation of the spindle checkpoint, or for the response of this checkpoint to elevated levels of Ran-GTP.

The Nup107-160 Complex Is Required for a Normal Spindle Assembly

Because the Nup107-160 complex did not seem to be required at kinetochores for the spindle checkpoint, we wondered whether it might play a role in spindle assembly. We used two experimental approaches to address this question. First, we assayed spindle assembly around sperm chromatin in Nup107-160 complex-depleted CSF extracts. Note that under these conditions, sperm chromatin has not undergone DNA replication before spindle assembly, so that it contains only unreplicated centromeres. Also, the sperm chromatin brings only one centriole pair into the reaction, so only a single pole is formed around a centrosome. The other pole is spontaneously formed in this reaction through the Ran-dependent nucleation of microtubules in the vicinity of the sperm chromatin (Mitchison *et al.*, 2004). We added sperm chromatin and rhodamine-labeled tubulin to mock- and Nup107-160 complex-depleted extracts and allowed spindle formation for 60 min. Abundant bipolar spindles formed throughout the mock-depleted mitotic extract at 60 min (Figure 6A, mock depleted). In strong contrast, only around 15% of the sperm chromatin in the depleted extracts was associated with spindles. Instead, most chromatin seemed rounded with few or no associated microtubules at 60 min (Figure 6A, Δ107-160). The rare bipolar spindles that we observed were faint and contained many fewer microtubules (Figure 6A, Δ107-160, right). These data indicate that the absence of the Nup107-160 complex severely disrupts spindle assembly.

In the second approach, we used "cycled" extracts, where chromosomes were fully replicated and centrosomes duplicated during interphase. The reactions were then driven

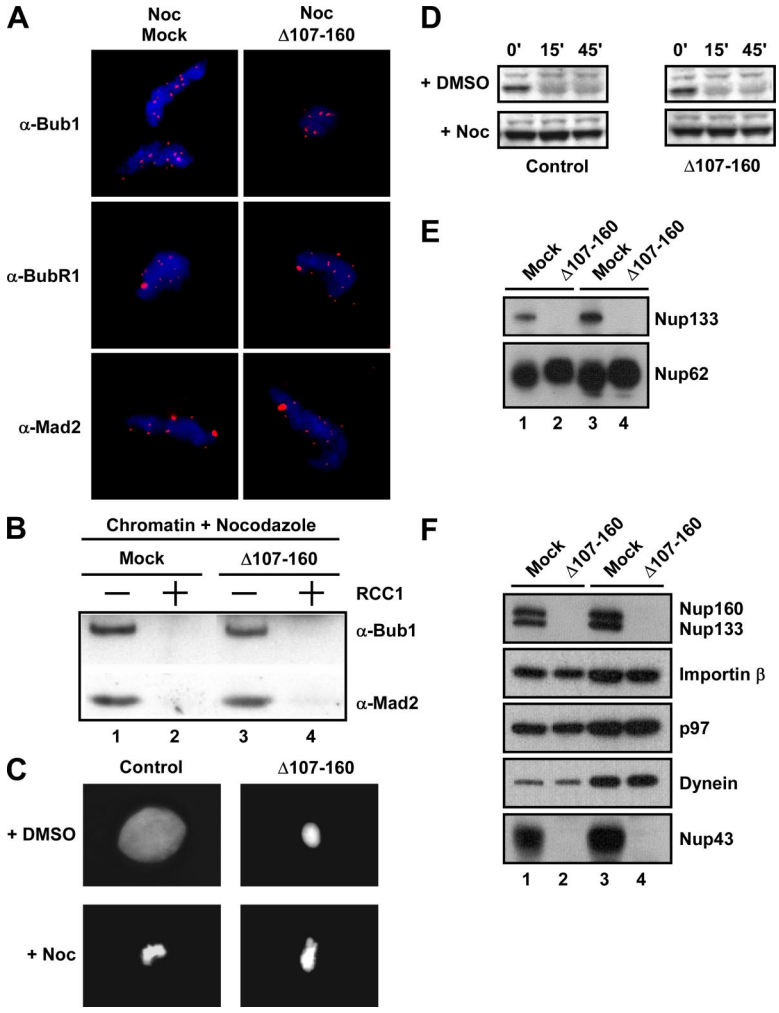

Figure 5. Extracts lacking the Nup107-160 complex have an intact spindle checkpoint. (A) Nup107-160 complex depleted (Δ107-160) or mock depleted (mock) CSF extracts plus sperm chromatin and nocodazole were incubated for 40 min at 23°C. Mitotic chromosomes were analyzed by indirect immunofluorescence by using antibodies to the checkpoint proteins Bub1, BubR1, and Mad2, which accumulated at kinetochores even in the absence of the Nup107-160 complex. (B) The checkpoint was checked for responsiveness to Ran by the addition of the RanGEF RCC1 (lanes 2 and 4). The checkpoint protein Bub1 and Mad2 were released normally in both extracts. (C) CSF extracts with nuclei were treated with DMSO (top) or nocodazole (bottom). After incubation for 40 min, extracts were stimulated with 0.6 mM Ca^{2+} to destroy CSF. At 45 min after calcium addition, Hoechst 33258 dye was added for the examination of DNA morphology. (D) At the indicated times after calcium addition aliquots were removed for Western blot analysis with anti-cyclin B2 antibodies. (E) Anti-Nup133 immunodepletion of mitotic CSF extract removes all visible Nup133 (lanes 2 and 4; 0.2 and 0.4 μl of extract was loaded, respectively). Mock depletion of extract with control IgG antibodies did not (lanes 1 and 3; 0.2 and 0.4 μl). Levels of noncomplex nucleoporins, such as Nup62, were not altered. (F) An immunoblot of mock- and Nup107-160 complex-depleted extracts is shown probed with antibodies to Nup160, Nup133, Importin-α, the AAA ATPase p97, dynein, and Nup43. Lanes 1 and 2 contain 0.2 μl of extract; lanes 3 and 4 contain 0.4 μl of extract. Nup160, Nup133, and Nup43, all members of the complex, were depleted. Levels of Importins and noncomplex kinetochore components tested were not altered by Nup107-160 deletion.

back into M phase through the addition of fresh CSF extract, as in Figure 3. Notably, it was not possible to perform this type of experiment using immunodepleted extracts, because both nuclear pore assembly and DNA replication are depen-

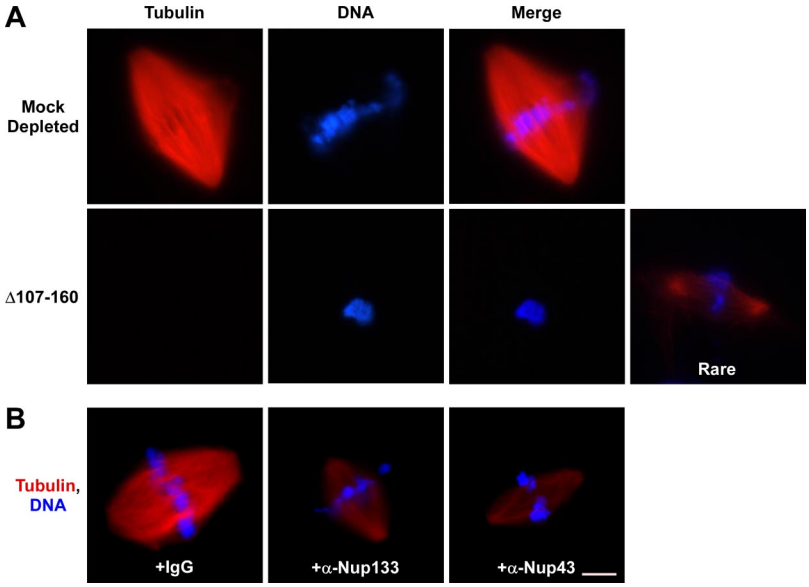

Figure 6. Disruption of the Nup107-160 complex severely compromises spindle assembly. (A) Spindles were assembled for 60 min in vitro by adding sperm chromatin and rhodamine-labeled tubulin to mitotic CSF extracts that were either mock-depleted (top) or Nup107-160 complex-depleted (bottom). Aliquots were examined for spindle assembly by fixation, centrifugation, and a second fixation, before examination with a Zeiss Axioskop fluorescence microscope. In both A and B, DNA was stained with DAPI DNA dye (blue, all rows). Absence of the Nup107-160 complex produced a much reduced number of bipolar spindles and those that were seen were small and contained many fewer microtubules. (B) Nuclei were assembled in interphase *Xenopus* extract for 60 min. At that time, an equal volume of CSF extract was added to convert the interphase extract to mitosis, via the cyclin B present in the CSF extract. Five minutes later rhodamine-labeled tubulin and either control IgG (left), affinity-purified anti-Nup133 antibody (middle), or affinity-purified anti-Nup43 antibody (right) were added. Spindle assembly was assessed 60 min later, as in A. Both antibodies to the Nup107-160 complex significantly interfered with correct spindle assembly, mirroring the depletion defect of A. Bar, 10 μm.

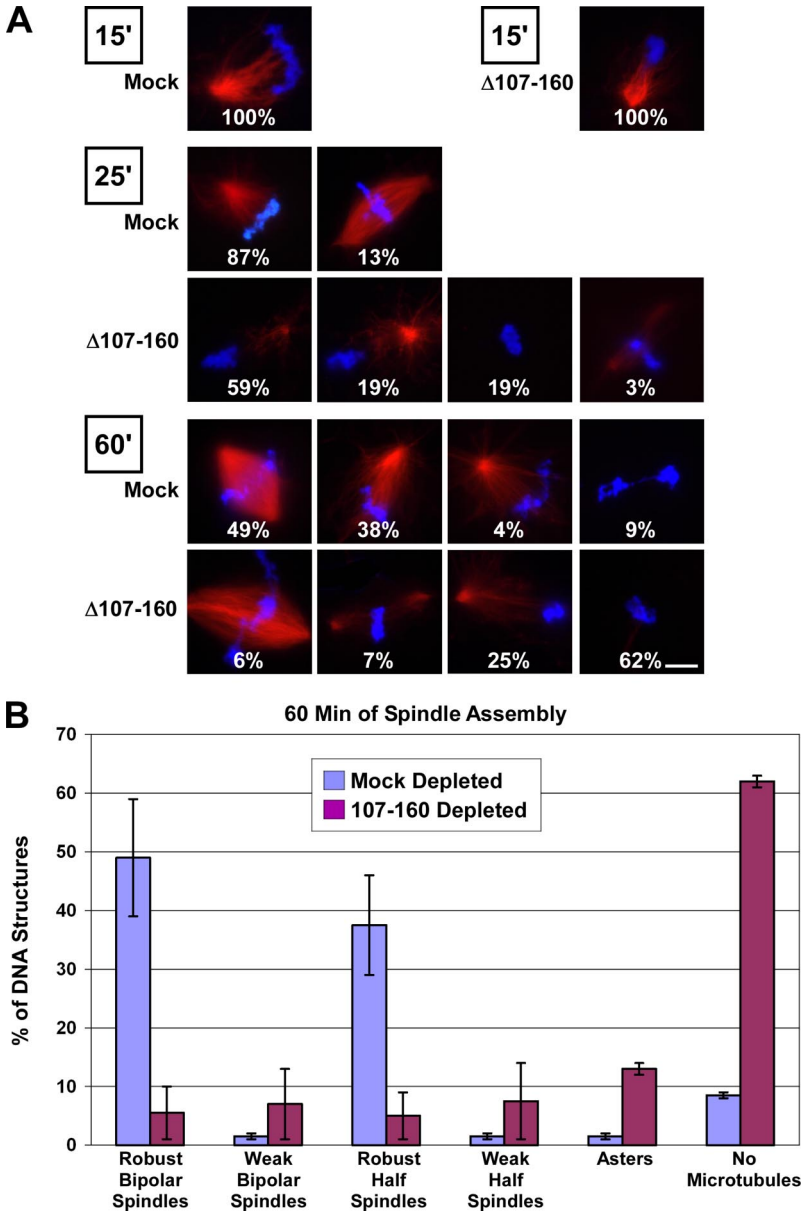

Figure 7. Absence of the Nup107-160 complex causes an increasing regression in spindle assembly and stability. (A) Mock-depleted and Nup107-160 complex-depleted *Xenopus* mitotic (CSF) extracts were supplemented with rhodamine-labeled tubulin and sperm chromatin at t = 0′. Aliquots were withdrawn at 15, 25, and 60 min, prefixed with formaldehyde, spun down onto coverslips, postfixed with methanol, and examined with a Zeiss Axioskop 2 microscope. Bar, 10 μm. (B) Quantitation of in vitro spindle defects observed upon depletion of the Nup107-160 complex. The data from the 60-min time point in Figure 7A is shown graphically.

dent upon the intact Nup107-160 complex (Harel *et al.*, 2003b). Instead, we added rhodamine-labeled tubulin 5 min after the induction of reentry into mitosis, along with a control IgG, affinity-purified anti-Nup133 antibody, or affinity-purified anti-Nup43 antibody (Figure 6B). Addition of antibodies at this point allowed us to restrict our analysis of Nup107-160 complex function strictly to mitosis. As before, the samples were fixed and centrifuged onto coverslips.

The control IgG-treated reaction showed normal, bipolar spindle formation (Figure 6B, left). By contrast, antibodies directed against either Nup133 and Nup43 significantly interfered with correct spindle assembly (Figure 6B; Supplemental Table 3). In this case, we found that faint spindles bipolar spindles were more common than chromatin completely devoid of microtubules. These spindles were greatly reduced in overall size and had a maximal density of spindle microtubules that was only one-half of the density found in IgG-treated controls. Together, both approaches lead us to conclude than the Nup107-160 complex is essential for robust mitotic spindle formation.

The Nup107-160 Complex Is Not Required for Ran Aster Assembly

Logically, the defects observed after Nup107-160 complex depletion could reflect disruption of several distinct processes required for spindle formation. These processes include microtubule polymerization, initial aster assembly around sperm centrioles, and kinetochore attachment. Under normal circumstances, increased levels of Ran-GTP cause massive polymerization of microtubules in mitotic *Xenopus* extracts, even in the absence of added chromatin (Kalab *et al.*, 1999; Ohba *et al.*, 1999; Wilde and Zheng, 1999; Zhang *et al.*, 1999). These asters spontaneously rearrange into spindle-like structures (microspindles) through the action of multiple microtubule motor proteins within extracts. To test whether Ran-mediated microtubule assembly path-

ways are disrupted by the absence of the Nup107-160 complex, we measured the capacity of Nup107-160-depleted mitotic extracts (Figure 5, E and F) to form microtubule asters and spindle-like structures in response to a constitutively GTP-bound form of Ran (Ran-Q69L; 25 μM, final). We added rhodamine-tubulin at the start of the reaction to visualize microtubule assembly and assayed aster assembly microscopically after 30 min.

As shown in Supplemental Figure 2, RanQ69L-induced asters formed equivalently in both mock- and Nup107-160 complex-depleted extracts (top). The morphology of asters in both reactions was very similar, and the number of asters in the Nup107-160-depleted extract (13 $\pm$ 6 asters/field) was comparable with or greater than the number in mock-depleted control reactions (11 $\pm$ 6 asters/field). Similarly, microspindles formed at least as well in Nup107-160-depleted extracts as in mock-depleted extracts (Supplemental Figure 2, bottom). We conclude that the Nup107-160 complex is not required for microtubule polymerization in response to elevated Ran-GTP levels.

The Nup107-160 Complex Is Required for Formation of a Stable Mitotic Spindle In Vitro

We next wished to ascertain whether formation of asters around sperm centrioles occurred normally as well as to determine when a clear spindle assembly defect could first be observed. To do this, we examined the time-course spindle assembly around sperm chromatin in control and Nup107-160-depleted CSF extracts (Figure 7).

After 15 min, each group of sperm chromosomes in both mock and depleted extracts was associated with a microtubule aster (Figure 7A). The size and morphology of these asters was comparable between the depleted and control reactions, although the size was perhaps slightly less in depleted reactions. This observation suggests that sperm aster formation initially occurs relatively normally in the absence of the Nup107-160 complex. After 25 min, the majority (87%) of chromatin figures in the mock-depleted extract had advanced to very robust half-spindles, and 13% were already bipolar (Figure 7, mock, 25′). However, the asters that had formed on chromatin in the Nup107-160-depleted extract at 15 min had deteriorated, such that 19% of the chromatin lacked any microtubules and 59% had few microtubules (Figure 7A, Δ107-160, 25′).

After 1 h, fully one-half of the sperm chromatin in the mock-depleted extract had formed robust bipolar spindles (Figure 7, A and B). In the depleted extract, however, the deterioration in microtubules had progressed further, such that a large fraction of the chromatin figures (62%) lacked any associated microtubules whatsoever. A small fraction of the sperm chromatin (~6%) was associated with bipolar spindles at this point. Interestingly, an increased intensity of DNA staining in most of these cases suggested that the few bipolar spindles found in depleted egg extracts may have formed predominately from fusion of two chromatin masses and their associated half-spindles. The data from the chromatin figures at the 60-min time point is summarized in Figure 7B. The endpoint of this kinetic experiment was entirely consistent with what we had observed in depletion of the Nup107-160 complex from mitotic extract (Figure 6A). Specifically, the majority of structures observed in Nup107-160 complex-depleted extracts were extremely thin in density of microtubules.

Together, our results argue that the Nup107-160 complex plays an important role in mitotic spindle assembly. Its function is not critical to microtubule nucleation around sperm centrosomes or for microtubule assembly in response to exogenous Ran-GTP. Rather, the defects in spindle assembly that we observe in the absence of the Nup107-160 complex arise at later times; these phenotypes are consistent with the notion that this complex is important for the assembly or maintenance of microtubule fibers between the spindle poles and chromosomes.

DISCUSSION

We have examined the localization and role of the Nup107-160 complex during mitosis. The Nup107-160 complex resembles a subset of checkpoint proteins in its bimodal distribution on spindles and kinetochores as well as in its dramatic accumulation on unattached kinetochores in nocodazole-treated cells. However, the Nup107-160 complex was not required for any aspect of spindle checkpoint function that we tested. Rather, depletion or inhibition of the Nup107-160 complex rendered spindle assembly strikingly defective. Together, these observations offer a global picture of the dynamics of the Nup107-160 complex during mitosis as well as the first evidence for its mitotic function that can be clearly distinguished from its interphase roles in NPC structure and nuclear transport.

Antibodies to four different members of the Nup107-160 complex stained spindle poles and proximal spindle microtubules in mammalian cells during prometaphase (Figure 2). This spindle pole localization diminished significantly in metaphase, suggesting that complex localization is dynamic. The strong staining of spindles in *Xenopus* mitotic extracts using antisera to multiple members of the Nup107-160 complex (Figure 3) is consistent with our results in mammalian cells. The disparity of Nup107-160 complex distribution in prometaphase mammalian cells and *Xenopus* extracts may reflect differing mechanisms of spindle assembly in these two systems as well as the meiotic nature of CSF extracts. In particular, *Xenopus* spindles rely more upon self-organization (i.e., chromatin-induced microtubules) than search-and-capture mechanisms that are essential in somatic cells (i.e., centrosome-nucleated microtubules) (Karsenti and Vernos, 2001; Gadde and Heald, 2004; Mitchison, 2005).

The localization of the Nup107-160 complex (Figure 2) was reminiscent of the behavior of spindle checkpoint proteins Mad1, Mad2, and Bub3 (Howell *et al*., 2004; Maiato *et al*., 2004). Moreover, like the checkpoint proteins, accumulation of the Nup107-160 complex at kinetochores responded dynamically to cell cycle conditions. On disruption of kinetochore–microtubule attachment with nocodazole, we observed increased amounts of the Nup107-160 complex on kinetochores (Figure 4). Indeed, the Nup107-160 complex assembles into expanded crescents and rings around each kinetochore. This increase mirrors the behavior of BubR1 and Mad2 as well as the outer kinetochore motor proteins dynein and CENP E (Hoffman *et al*., 2001; Maiato *et al*., 2004). A notable difference, however, is that the Nup107-160 complex remains on kinetochores through anaphase (Figure 2A; Loiodice *et al*., 2004), whereas Mad1, Mad2, and Bub3 all become drastically reduced after kinetochore–microtubule attachment (Taylor *et al*., 1998; Shannon *et al*., 2002; Howell *et al*., 2004). Therefore, checkpoint proteins and the Nup107-160 complex diverge in their behavior during later stages of mitosis.

Despite similarities in behavior of checkpoint proteins and of the Nup107-160 complex, we did not find that this complex is essential for the correct localization of checkpoint proteins to kinetochores in egg extracts, for the activation of the spindle checkpoint or for the regulation of this checkpoint by Ran-GTP (Figure 5). Our findings cannot not rule

out, however, the possibility that a very small amount of Nup107-160 complex remains in the depleted extract, sufficient for activation of the highly sensitive spindle checkpoint.

The Nup107-160 complex was similarly dispensable for formation of microtubule asters around sperm centrioles (Figure 7A), and for formation of asters in response to exogenous Ran-GTP (Supplemental Figure 2). By contrast to the Nup107-160 complex, the mRNA export factor Rae1 is essential in *Xenopus* extracts for assembly of Ran-GTP asters and spindles associated with sperm chromatin (Blower *et al*., 2005). This difference between Rae1- and Nup107-160–depleted extracts suggests that the Nup107-160 complex acts either distinctly from or upstream of Rae1. Ran-GTP-induced asters in extracts depleted of the Nup107-160 complex eventually organized into microspindles (Supplemental Figure 2), further indicating that this complex is not required for motor activities involved in microspindles formation (Karsenti and Vernos, 2001; Gadde and Heald, 2004; Mitchison, 2005).

However, our study revealed that the Nup107-160 complex is critical for later events in spindle assembly around chromatin in both CSF extracts (Figures 6 and 7) and cycled extracts (Figure 6). Our data would be consistent with the possibility that the Nup107-160 complex acts directly in these later steps of spindle assembly. Possibly more likely, however, the complex might also function indirectly, through intimate association to or regulatory interaction with other spindle- or kinetochore-associated proteins. Interestingly, the defects observed in Nup107-160-depleted egg extracts were reminiscent of defects in egg extracts depleted of the chromosomal passenger complex (CPC), which also show aster assembly around sperm centrioles, but do not progress to formation of bipolar spindles (Sampath *et al*., 2004). The possible relationship of the Nup107-160 complex to the CPC and other established spindle assembly factors will be an interesting topic for future investigation.

Our results do not provide a definitive point of action for the complex at later stages of spindle assembly. However, detailed reports on spindle assembly in egg extracts allow some speculation on this topic. Each group of sperm chromosomes initially forms a pole around their single centrosome when added to CSF egg extracts, and the second pole is subsequently derived from chromosomally stabilized microtubules (Mitchison *et al*., 2004). It has been well established that the localized production of Ran-GTP by RCC1 contributes substantially to chromatin-induced microtubule assembly (Hetzer *et al*., 2002). The flux of spindle microtubules commences when bipolarity is achieved in this manner, presumably in response to the assembly of antiparallel, overlapping microtubules originating at the opposite poles (Mitchison *et al*., 2004). Notably, sequestration of Ran pathway targets by exogenous Importin-α causes a loss of microtubule density in preformed spindles and blocks spindle microtubule flux. Based upon these observations and findings in other systems, we can imagine two possible roles for the Nup107-160 complex, which are not mutually exclusive.

In the first model, the absence of the Nup107-160 complex on kinetochores may be causative for the defects we observed. In this case, depletion of the Nup107-160 complex may prevent effective capture of centrosome-initiated microtubules, which is known to be required for production of stable spindle fibers. Indeed, both the kinetochore localization of the Nup107-160 complex and the normal initiation but subsequent decay of centrosome-induced asters in Nup107-160 complex-depleted extracts might be consistent with an inability of kinetochores to capture and stabilize microtubules. Alternatively, the Nup107-160 complex may play a general role in stabilizing spindle microtubules around sperm chromatin, perhaps by acting as an upstream regulator of the Ran pathway. In this case, monopolar spindles would fail to mature into bipolar structures around chromatin added to CSF extracts and would not develop networks of antiparallel microtubules required to promote flux within the spindle. This model might account for the persistence of weak bipolar spindles in the cycled extracts; each group of chromosomes in this situation would form spindles containing two centrosomes and might therefore be less dependent upon chromatin-mediated stabilization of microtubules for achieving bipolar organization.

In summary, Nup107-160 complex localization on spindles mirrors the behavior of a subset of spindle checkpoint proteins, both in occurring transiently in the spindle pole at prometaphase and in responding dynamically to spindle checkpoint conditions at the kinetochore. Within mitosis, this complex has a role in spindle assembly that can be clearly distinguished from interphase nuclear envelope assembly and NPC function. This complex is therefore likely to be important for accurate mitotic segregation of vertebrate chromosomes.

ACKNOWLEDGMENTS

We thank A. Desai and D. Cleveland for helpful comments. This work was supported by National Institutes of Health Grant R01 GM-33279 to D. F. and by Intramural National Institute of Child Health and Human Development funds to M. D.

REFERENCES

Aitchison, J. D., Blobel, G., and Rout, M. P. (1995). Nup120p: a yeast nucleoporin required for NPC distribution and mRNA transport. J. Cell Biol. *131*, 1659–1675.

Arnaoutov, A., Azuma, Y., Ribbeck, K., Joseph, J., Boyarchuk, Y., Karpova, T., McNally, J., and Dasso, M. (2005). Crm1 is a mitotic effector of Ran-GTP in somatic cells. Nat. Cell Biol. *7*, 626–632.

Arnaoutov, A., and Dasso, M. (2003). The Ran GTPase regulates kinetochore function. Dev. Cell *5*, 99–111.

Askjaer, P., Galy, V., Hannak, E., and Mattaj, I. W. (2002). Ran GTPase cycle and importins alpha and beta are essential for spindle formation and nuclear envelope assembly in living *Caenorhabditis elegans* embryos. Mol. Biol. Cell *13*, 4355–4370.

Bai, S. W., Rouquette, J., Umeda, M., Faigle, W., Loew, D., Sazer, S., and Doye, V. (2004). The fission yeast Nup107-120 complex functionally interacts with the small GTPase Ran/Spi1 and is required for mRNA export, nuclear pore distribution, and proper cell division. Mol. Cell. Biol. *24*, 6379–6392.

Bamba, C., Bobinnec, Y., Fukuda, M., and Nishida, E. (2002). The GTPase Ran regulates chromosome positioning and nuclear envelope assembly in vivo. Curr. Biol. *12*, 503–507.

Belgareh, N. *et al*. (2001). An evolutionarily conserved NPC subcomplex, which redistributes in part to kinetochores in mammalian cells. J. Cell Biol. *154*, 1147–1160.

Belgareh, N., Snay-Hodge, C., Pasteau, F., Dagher, S., Cole, C. N., and Doye, V. (1998). Functional characterization of a Nup159p-containing nuclear pore subcomplex. Mol. Biol. Cell *9*, 3475–3492.

Blower, M. D., Nachury, M., Heald, R., and Weis, K. (2005). A Rae1-containing ribonucleoprotein complex is required for mitotic spindle assembly. Cell *121*, 223–234.

Boehmer, T., Enninga, J., Dales, S., Blobel, G., and Zhong, H. (2003). Depletion of a single nucleoporin, Nup107, prevents the assembly of a subset of nucleoporins into the nuclear pore complex. Proc. Natl. Acad. Sci. USA *100*, 981–985.

Campbell, M. S., Chan, G. K., and Yen, T. J. (2001). Mitotic checkpoint proteins HsMAD1 and HsMAD2 are associated with nuclear pore complexes in interphase. J. Cell Sci. *114*, 953–963.

Carazo-Salas, R. E., Guarguaglini, G., Gruss, O. J., Segref, A., Karsenti, E., and Mattaj, I. W. (1999). Generation of GTP-bound Ran by RCC1 is required for chromatin-induced mitotic spindle formation. Nature *400*, 178–181.

Caudron, M., Bunt, G., Bastiaens, P., and Karsenti, E. (2005). Spatial coordination of spindle assembly by chromosome-mediated signaling gradients. Science *309*, 1373–1376.

Clarke, P. R. (2005). Cell biology. A gradient signal orchestrates the mitotic spindle. Science *309*, 1334–1335.

Cronshaw, J. M., Krutchinsky, A. N., Zhang, W., Chait, B. T., and Matunis, M. J. (2002). Proteomic analysis of the mammalian nuclear pore complex. J. Cell Biol. *158*, 915–927.

Desai, A., Murray, A., Mitchison, T. J., and Walczak, C. E. (1999). The use of *Xenopus* egg extracts to study mitotic spindle assembly and function in vitro. Methods Cell Biol. *61*, 385–412.

Devos, D., Dokudovskaya, S., Alber, F., Williams, R., Chait, B. T., Sali, A., and Rout, M. P. (2004). Components of coated vesicles and nuclear pore complexes share a common molecular architecture. PLoS Biol. *2*, e380

Di Fiore, B., Ciciarello, M., and Lavia, P. (2004). Mitotic functions of the Ran GTPase network: the importance of being in the right place at the right time. Cell Cycle *3*, 305–313.

Di Fiore, B., Ciciarello, M., Mangiacasale, R., Palena, A., Tassin, A. M., Cundari, E., and Lavia, P. (2003). Mammalian RanBP1 regulates centrosome cohesion during mitosis. J. Cell Sci. *116*, 3399–3411.

Doye, V., Wepf, R., and Hurt, E. C. (1994). A novel nuclear pore protein Nup133p with distinct roles in poly(A)+ RNA transport and nuclear pore distribution. EMBO J. *13*, 6062–6075.

Ems-McClung, S. C., Zheng, Y., and Walczak, C. E. (2004). Importin alpha/beta and Ran-GTP regulate XCTK2 microtubule binding through a bipartite nuclear localization signal. Mol. Biol. Cell *15*, 46–57.

Enninga, J., Levay, A., and Fontoura, B. M. (2003). Sec13 shuttles between the nucleus and the cytoplasm and stably interacts with Nup96 at the nuclear pore complex. Mol. Cell. Biol. *23*, 7271–7284.

Fontoura, B. M., Blobel, G., and Matunis, M. J. (1999). A conserved biogenesis pathway for nucleoporins: proteolytic processing of a 186-kilodalton precursor generates Nup98 and the novel nucleoporin, Nup96. J. Cell Biol. *144*, 1097–1112.

Gadde, S., and Heald, R. (2004). Mechanisms and molecules of the mitotic spindle. Curr. Biol. *14*, R797–R805.

Goldstein, A. L., Snay, C. A., Heath, C. V., and Cole, C. N. (1996). Pleiotropic nuclear defects associated with a conditional allele of the novel nucleoporin Rat9p/Nup85p. Mol. Biol. Cell *7*, 917–934.

Gruss, O. J., Carazo-Salas, R. E., Schatz, C. A., Guarguaglini, G., Kast, J., Wilm, M., Le Bot, N., Vernos, I., Karsenti, E., and Mattaj, I. W. (2001). Ran induces spindle assembly by reversing the inhibitory effect of importin alpha on TPX2 activity. Cell *104*, 83–93.

Harel, A., Chan, R. C., Lachish-Zalait, A., Zimmerman, E., Elbaum, M., and Forbes, D. J. (2003a). Importin beta negatively regulates nuclear membrane fusion and nuclear pore complex assembly. Mol. Biol. Cell *14*, 4387–4396.

Harel, A., and Forbes, D. J. (2004). Importin beta: conducting a much larger cellular symphony. Mol. Cell *16*, 319–330.

Harel, A., Orjalo, A. V., Vincent, T., Lachish-Zalait, A., Vasu, S., Shah, S., Zimmerman, E., Elbaum, M., and Forbes, D. J. (2003b). Removal of a single pore subcomplex results in vertebrate nuclei devoid of nuclear pores. Mol. Cell *11*, 853–864.

Heald, R., Tournebize, R., Blank, T., Sandaltzopoulos, R., Becker, P., Hyman, A., and Karsenti, E. (1996). Self-organization of microtubules into bipolar spindles around artificial chromosomes in *Xenopus* egg extracts. Nature *382*, 420–425.

Heath, C. V., Copeland, C. S., Amberg, D. C., Del Priore, V., Snyder, M., and Cole, C. N. (1995). Nuclear pore complex clustering and nuclear accumulation of poly(A)+ RNA associated with mutation of the *Saccharomyces cerevisiae* RAT2/NUP120 gene. J. Cell Biol. *131*, 1677–1697.

Hetzer, M., Bilbao-Cortes, D., Walther, T. C., Gruss, O. J., and Mattaj, I. W. (2000). GTP hydrolysis by Ran is required for nuclear envelope assembly. Mol. Cell *5*, 1013–1024.

Hetzer, M., Gruss, O. J., and Mattaj, I. W. (2002). The Ran GTPase as a marker of chromosome position in spindle formation and nuclear envelope assembly. Nat. Cell Biol. *4*, E177–E184.

Hetzer, M. W., Walther, T. C., and Mattaj, I. W. (2005). Pushing the envelope: structure, function, and dynamics of the nuclear periphery. Annu. Rev. Cell Dev. Biol. *21*, 347–380.

Hoffman, D. B., Pearson, C. G., Yen, T. J., Howell, B. J., and Salmon, E. D. (2001). Microtubule-dependent changes in assembly of microtubule motor proteins and mitotic spindle checkpoint proteins at PtK1 kinetochores. Mol. Biol. Cell *12*, 1995–2009.

Howell, B. J., Moree, B., Farrar, E. M., Stewart, S., Fang, G., and Salmon, E. D. (2004). Spindle checkpoint protein dynamics at kinetochores in living cells. Curr. Biol. *14*, 953–964.

Iouk, T., Kerscher, O., Scott, R. J., Basrai, M. A., and Wozniak, R. W. (2002). The yeast nuclear pore complex functionally interacts with components of the spindle assembly checkpoint. J. Cell Biol. *159*, 807–819.

Jeganathan, K. B., Malureanu, L., and van Deursen, J. M. (2005). The Rae1-Nup98 complex prevents aneuploidy by inhibiting securin degradation. Nature *438*, 1036–1039.

Joseph, J., Liu, S. T., Jablonski, S. A., Yen, T. J., and Dasso, M. (2004). The RanGAP1-RanBP2 complex is essential for microtubule-kinetochore interactions in vivo. Curr. Biol. *14*, 611–617.

Joseph, J., Tan, S. H., Karpova, T. S., McNally, J. G., and Dasso, M. (2002). SUMO-1 targets RanGAP1 to kinetochores and mitotic spindles. J. Cell Biol. *156*, 595–602.

Kalab, P., Pu, R. T., and Dasso, M. (1999). The ran GTPase regulates mitotic spindle assembly. Curr. Biol. *9*, 481–484.

Kalab, P., Weis, K., and Heald, R. (2002). Visualization of a Ran-GTP gradient in interphase and mitotic *Xenopus* egg extracts. Science *295*, 2452–2456.

Karsenti, E., and Vernos, I. (2001). The mitotic spindle: a self-made machine. Science *294*, 543–547.

Kastenmayer, J. P., Lee, M. S., Hong, A. L., Spencer, F. A., and Basrai, M. A. (2005). The C-terminal half of *Saccharomyces cerevisiae* Mad1p mediates spindle checkpoint function, chromosome transmission fidelity and CEN association. Genetics *170*, 509–517.

Keryer, G., Di Fiore, B., Celati, C., Lechtreck, K. F., Mogensen, M., Delouvee, A., Lavia, P., Bornens, M., and Tassin, A. M. (2003). Part of Ran is associated with AKAP450 at the centrosome: involvement in microtubule-organizing activity. Mol. Biol. Cell *14*, 4260–4271.

Kraemer, D., Dresbach, T., and Drenckhahn, D. (2001). Mrnp41 (Rae 1p) associates with microtubules in HeLa cells and in neurons. Eur. J. Cell Biol. *80*, 733–740.

Kutay, U., Izaurralde, E., Bischoff, F. R., Mattaj, I. W., and Gorlich, D. (1997). Dominant-negative mutants of importin-beta block multiple pathways of import and export through the nuclear pore complex. EMBO J. *16*, 1153–1163.

Li, H. Y., and Zheng, Y. (2004). Phosphorylation of RCC1 in mitosis is essential for producing a high RanGTP concentration on chromosomes and for spindle assembly in mammalian cells. Genes Dev. *18*, 512–527.

Li, O., Heath, C. V., Amberg, D. C., Dockendorff, T. C., Copeland, C. S., Snyder, M., and Cole, C. N. (1995). Mutation or deletion of the *Saccharomyces cerevisiae* RAT3/NUP133 gene causes temperature-dependent nuclear accumulation of poly(A)+ RNA and constitutive clustering of nuclear pore complexes. Mol. Biol. Cell *6*, 401–417.

Liu, S. T., Chan, G. K., Hittle, J. C., Fujii, G., Lees, E., and Yen, T. J. (2003). Human MPS1 kinase is required for mitotic arrest induced by the loss of CENP-E from kinetochores. Mol. Biol. Cell *14*, 1638–1651.

Loiodice, I., Alves, A., Rabut, G., Van Overbeek, M., Ellenberg, J., Sibarita, J. B., and Doye, V. (2004). The entire Nup107-160 complex, including three new members, is targeted as one entity to kinetochores in mitosis. Mol. Biol. Cell *15*, 3333–3344.

Lutzmann, M., Kunze, R., Buerer, A., Aebi, U., and Hurt, E. (2002). Modular self-assembly of a Y-shaped multiprotein complex from seven nucleoporins. EMBO J *21*, 387–397.

Macara, I. G. (2001). Transport into and out of the nucleus. Microbiol. Mol. Biol. Rev. *65*, 570–594, table of contents.

Maiato, H., DeLuca, J., Salmon, E. D., and Earnshaw, W. C. (2004). The dynamic kinetochore-microtubule interface. J. Cell Sci. *117*, 5461–5477.

Merdes, A., Ramyar, K., Vechio, J. D., and Cleveland, D. W. (1996). A complex of NuMA and cytoplasmic dynein is essential for mitotic spindle assembly. Cell *87*, 447–458.

Minshull, J., Sun, H., Tonks, N. K., and Murray, A. W. (1994). A MAP kinase-dependent spindle assembly checkpoint in *Xenopus* egg extracts. Cell *79*, 475–486.

Mitchison, T. J. (2005). Mechanism and function of poleward flux in *Xenopus* extract meiotic spindles. Philos. Trans. R. Soc. Lond. B. Biol. Sci. *360*, 623–629.

Mitchison, T. J., Maddox, P., Groen, A., Cameron, L., Perlman, Z., Ohi, R., Desai, A., Salmon, E. D., and Kapoor, T. M. (2004). Bipolarization and poleward flux correlate during *Xenopus* extract spindle assembly. Mol. Biol. Cell *15*, 5603–5615.

Murray, A. W. (1991). Cell cycle extracts. Methods Cell Biol. *36*, 581–605.

Nachury, M. V., Maresca, T. J., Salmon, W. C., Waterman-Storer, C. M., Heald, R., and Weis, K. (2001). Importin beta is a mitotic target of the small GTPase Ran in spindle assembly. Cell *104*, 95–106.

Ohba, T., Nakamura, M., Nishitani, H., and Nishimoto, T. (1999). Self-organization of microtubule asters induced in *Xenopus* egg extracts by GTP-bound Ran. Science *284*, 1356–1358.

Pemberton, L. F., Rout, M. P., and Blobel, G. (1995). Disruption of the nucleoporin gene NUP133 results in clustering of nuclear pore complexes. Proc. Natl. Acad. Sci. USA *92*, 1187–1191.

Quimby, B. B., Arnaoutov, A., and Dasso, M. (2005). Ran GTPase regulates Mad2 localization to the nuclear pore complex. Eukaryot. Cell *4*, 274–280.

Salina, D., Enarson, P., Rattner, J. B., and Burke, B. (2003). Nup358 integrates nuclear envelope breakdown with kinetochore assembly. J. Cell Biol. *162*, 991–1001.

Sampath, S. C., Ohi, R., Leismann, O., Salic, A., Pozniakovski, A., and Funabiki, H. (2004). The chromosomal passenger complex is required for chromatin-induced microtubule stabilization and spindle assembly. Cell *118*, 187–202.

Shah, S., Tugendreich, S., and Forbes, D. (1998). Major binding sites for the nuclear import receptor are the internal nucleoporin Nup153 and the adjacent nuclear filament protein Tpr. J. Cell Biol. *141*, 31–49.

Shannon, K. B., Canman, J. C., and Salmon, E. D. (2002). Mad2 and BubR1 function in a single checkpoint pathway that responds to a loss of tension. Mol. Biol. Cell *13*, 3706–3719.

Siniossoglou, S., Lutzmann, M., Santos-Rosa, H., Leonard, K., Mueller, S., Aebi, U., and Hurt, E. (2000). Structure and assembly of the Nup84p complex. J. Cell Biol. *149*, 41–54.

Siniossoglou, S., Wimmer, C., Rieger, M., Doye, V., Tekotte, H., Weise, C., Emig, S., Segref, A., and Hurt, E. C. (1996). A novel complex of nucleoporins, which includes Sec13p and a Sec13p homolog, is essential for normal nuclear pores. Cell *84*, 265–275.

Stukenberg, P. T., and Macara, I. G. (2003). The kinetochore NUPtials. Nat. Cell Biol. *5*, 945–947.

Suntharalingam, M., and Wente, S. R. (2003). Peering through the pore: nuclear pore complex structure, assembly, and function. Dev. Cell *4*, 775–789.

Taylor, S. S., Ha, E., and McKeon, F. (1998). The human homologue of Bub3 is required for kinetochore localization of Bub1 and a Mad3/Bub1-related protein kinase. J. Cell Biol. *142*, 1–11.

Teixeira, M. T., Siniossoglou, S., Podtelejnikov, S., Benichou, J. C., Mann, M., Dujon, B., Hurt, E., and Fabre, E. (1997). Two functionally distinct domains generated by in vivo cleavage of Nup145p: a novel biogenesis pathway for nucleoporins. EMBO J. *16*, 5086–5097.

Trieselmann, N., Armstrong, S., Rauw, J., and Wilde, A. (2003). Ran modulates spindle assembly by regulating a subset of TPX2 and Kid activities including Aurora A activation. J. Cell Sci. *116*, 4791–4798.

Trieselmann, N., and Wilde, A. (2002). Ran localizes around the microtubule spindle in vivo during mitosis in *Drosophila* embryos. Curr. Biol. *12*, 1124–1129.

Tsai, M. Y., Wiese, C., Cao, K., Martin, O., Donovan, P., Ruderman, J., Prigent, C., and Zheng, Y. (2003). A Ran signalling pathway mediated by the mitotic kinase Aurora A in spindle assembly. Nat. Cell Biol. *5*, 242–248.

Vasu, S., Shah, S., Orjalo, A., Park, M., Fischer, W. H., and Forbes, D. J. (2001). Novel vertebrate nucleoporins Nup133 and Nup160 play a role in mRNA export. J. Cell Biol. *155*, 339–354.

Vasu, S. K., and Forbes, D. J. (2001). Nuclear pores and nuclear assembly. Curr. Opin. Cell Biol. *13*, 363–375.

Walther, T. C., *et al*. (2003a). The conserved Nup107-160 complex is critical for nuclear pore complex assembly. Cell *113*, 195–206.

Walther, T. C., Askjaer, P., Gentzel, M., Habermann, A., Griffiths, G., Wilm, M., Mattaj, I. W., and Hetzer, M. (2003b). RanGTP mediates nuclear pore complex assembly. Nature *424*, 689–694.

Whalen, W. A., Bharathi, A., Danielewicz, D., and Dhar, R. (1997). Advancement through mitosis requires rae1 gene function in fission yeast. Yeast *13*, 1167–1179.

Wiese, C., Wilde, A., Moore, M. S., Adam, S. A., Merdes, A., and Zheng, Y. (2001). Role of importin-beta in coupling Ran to downstream targets in microtubule assembly. Science *291*, 653–656.

Wilde, A., and Zheng, Y. (1999). Stimulation of microtubule aster formation and spindle assembly by the small GTPase Ran. Science *284*, 1359–1362.

Zhang, C., and Clarke, P. R. (2000). Chromatin-independent nuclear envelope assembly induced by Ran GTPase in *Xenopus* egg extracts. Science *288*, 1429–1432.

Zhang, C., and Clarke, P. R. (2001). Roles of Ran-GTP and Ran-GDP in precursor vesicle recruitment and fusion during nuclear envelope assembly in a human cell-free system. Curr. Biol. *11*, 208–212.

Zhang, C., Hughes, M., and Clarke, P. R. (1999). Ran-GTP stabilises microtubule asters and inhibits nuclear assembly in *Xenopus* egg extracts. J. Cell Sci. *112*, 2453–2461.